mAbs 7:1, 53–65; January/February 2015; Published with license by Taylor & Francis Group, LLC

Nanocell targeting using engineered bispecific antibodies

Karin Taylor[1,*], Christopher B Howard[1], Martina L Jones[1], Ilya Sedliarou[2], Jennifer MacDiarmid[2], Himanshu Brahmbhatt[2], Trent P Munro[1], and Stephen M Mahler[1,3]

[1]Australian Institute for Bioengineering and Nanotechnology (AIBN); University of Queensland, St Lucia; Queensland, Australia; [2]EnGeneIC Ltd; New South Wales, Australia; [3]School of Chemical Engineering; University of Queensland, St Lucia; Queensland, Australia

Keywords: bispecific antibody, disulfide bridge, mammalian expression, nanoparticle, single chain Fv, surface plasmon resonance, tumor regression

Abbreviations: BsAb, bispecific antibody; EDV^{TM}, EnGeneIC Delivery Vehicle; scFv, single chain variable fragment; EGFR, epidermal growth factor receptor; LPS, lipopolysaccharide; IgG, immunoglobulin G; mAb, monoclonal antibody; NP, nanoparticle

There are many design formats for bispecific antibodies (BsAbs), and the best design choice is highly dependent on the final application. Our aim was to engineer BsAbs to target a novel nanocell (EnGeneIC Delivery Vehicle or EDV^{TM}nanocell) to the epidermal growth factor receptor (EGFR). EDV^{TM}nanocells are coated with lipopolysaccharide (LPS), and BsAb designs incorporated single chain Fv (scFv) fragments derived from an anti-LPS antibody (1H10) and an anti-EGFR antibody, ABX-EGF. We engineered various BsAb formats with monovalent or bivalent binding arms and linked scFv fragments via either glycine-serine (G4S) or Fc-linkers. Binding analyses utilizing ELISA, surface plasmon resonance, bio-layer interferometry, flow cytometry and fluorescence microscopy showed that binding to LPS and to either soluble recombinant EGFR or MDA-MB-468 cells expressing EGFR, was conserved for all construct designs. However, the Fc-linked BsAbs led to nanocell clumping upon binding to EDV^{TM}nanocells. Clumping was eliminated when additional disulfide bonds were incorporated into the scFv components of the BsAbs, but this resulted in lower BsAb expression. The G4S-linked tandem scFv BsAb format was the optimal design with respect to EDV binding and expression yield. Doxorubicin-loaded EDV^{TM}nanocells actively targeted with tandem scFv BsAb in vivo to MDA-MB-468-derived tumors in mouse xenograft models enhanced tumor regression by 40% compared to passively targeted EDV^{TM}nanocells. BsAbs therefore provide a functional means to deliver EDV^{TM}nanocells to target cells.

Introduction

Therapeutic monoclonal antibodies (mAbs) approved for clinical use, such as bevacizumab (Avastin®), adalimumab (Humira®), trastuzumab (Herceptin®), cetuximab (Erbitux®) and panitumumab (Vectibix®), comprise a significant portion of the global pharmaceutical market.[1,2] Of the total mAb sales in 2010, half were attributed to cancer-related therapies.[3] In 2012, half of the antibody-based oncology products under clinical evaluation were full-length IgG mAbs, while the remaining candidates included drug-conjugated or radio-labeled mAbs, protein- and glyco-engineered mAbs and fragment or domain antibodies.[4–6] Also under evaluation are bispecific antibodies (BsAbs)[7], which are subject to increasing interest in recent years owing to their ability to target multiple antigens.[8-11]

BsAbs are able to crosslink antigenic determinants and so have value beyond that of single antigen-specific mAbs (**Fig. 1**).[1,11-15] The most prominent therapeutic utility for BsAbs in cancer therapeutics is the cross-linking of cell-surface antigens or receptors, so that immune cells can be tethered to cancer cells through a bispecific antibody.[9,11,12,16,17] Catumaxomab (Removab) was approved for therapeutic use in Europe in 2009, and remains the only approved therapeutic BsAb, although the number of BsAb formats entering clinical trials is increasing steadily.[7, 13] Catumaxomab is a T-cell engager, with specificity for both CD3 on cytotoxic T cells and the EpCAM antigen on ovarian cancer cells, for the treatment of malignant ascites.[18-20] Another emerging application of BsAbs is active targeting of drug-loaded nanoparticles (NP) to tumor sites by cross-linking the NP to tumor cells, leading to endocytosis, fusion with lysosomes and drug release intracellularly.[1,11,21,22]

The concept of NP-mediated drug delivery is attractive as it can lead to improvement in drug safety and efficacy. A myriad of engineered NPs for drug delivery have been developed, and include liposomes, polymeric-based NPs, silica, carbon, metal

*Correspondence to: Karin Taylor; Email: karin.taylor@uq.edu.au
Submitted: 09/29/2014; Revised: 10/29/2014; Accepted: 11/04/2014
http://dx.doi.org/10.4161/19420862.2014.985952

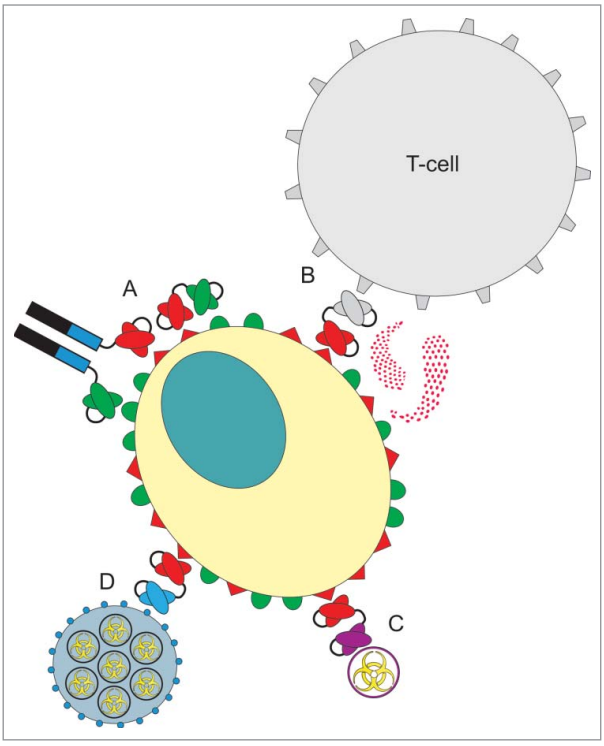

Figure 1. Applications of bispecific antibodies. Therapeutic modalities include: (**A**) crosslinking separate antigens on the cell surface; (**B**) T cell engagement by cross-linking CD3 on cytotoxic T cells to tumor cells; (**C**) targeting drugs or radiolabels to cell surface; (**D**) targeted delivery of drug-loaded nanoparticles to tumor cells (image not to scale).

oxides and other materials. Some are also derived from bacteria, viruses (e.g., virus-like particles) and eukaryotic cells (exosomes).[23-30] Advantages of NP-mediated drug delivery include protection of payloads such as DNA and RNA from degradation, improved drug pharmacokinetics and the enabling of effective drug dosing where drugs are insoluble.[2, 31] Notwithstanding the large number of NPs that have been developed for therapeutic application, at present there are only 7 nanomedicines approved for cancer therapy. All these nanomedicines operate through passive targeting, i.e., enhanced extravasation of NPs at the tumor site, facilitated by poorly differentiated tumor vasculature. There are a number of nanomedicines presently in clinical trials, with several of these targeted by antibodies.[32, 33]

NPs can carry drug payloads that include small molecule drugs, DNA or RNA.[2,30,34] Accumulation of the NPs at the tumor site by passive targeting decreases biodistribution, ideally localizing the therapeutic effects of the drug payload at the tumor site(s).[35, 36] Delivery of drugs sequestered within or attached to NPs opens the drug therapeutic window and addresses the low therapeutic index of free-drug administration, i.e., systemic drug delivery at required therapeutic doses results in acute toxicity and can elicit severe patient side effects. Furthermore, multiple drug resistance (MDR) can be alleviated by packaging NPs with siRNA or shRNA capable of interfering with cellular mechanisms promoting MDR.[22, 31]

For active targeting of NPs to tumor cells with antibodies, anti-tumor mAbs can be chemically conjugated to the NP, or alternatively be tethered to the NPs by using BsAbs that simultaneously bind the NP and the tumor target antigen.[37, 38] BsAbs can be produced by chemical conjugation of 2 mAbs or fragments with different specificities (e.g., via bis-maleimide cross-linking through Thiomab technology)[39] or alternatively via an affinity ligand such as Protein A or Protein G.[21] However, these methods can be associated with antibody inactivation, low yields and product heterogeneity; for example, yields of 10 - 40% dimeric BsAb from hetero-bifunctional reagents and 65 - 75% from homo-bifunctional reagents.[39] These methods rely on heterodimeric association of 2 mAbs. However homodimers can also be produced, limiting the yield of functional product.[40, 41]

Another method to construct BsAbs is to combine binding moieties such as scFvs or single domain antibodies into a single recombinant polypeptide chain using linkers such as the flexible glycine-serine (G4S) motif [9,10,17] or Fc (Hinge-CH2-CH3) domain. Improved scFv stability can be achieved through engineering additional cysteine residues within framework regions.[41] The modular design of recombinant BsAbs has resulted in the creation of a variety of novel BsAbs.[14] Formats range from non-IgG like varieties containing chemical or protein linkers, through to recombinant Fc-containing, Dock-and-lock and knobs-into-holes (KIH) BsAbs.[42] Some of the more well-known formats include Triomabs, dual affinity retargeting (DART) molecules, bispecific T-cell engagers (BiTEs), and the F-star mAb^{2TM} BsAbs.[9,20,43-45] Design features may endow the BsAb with specific properties, such as enhanced serum half-life or complement activation, by fusion with PEG, BSA or Fc domains.[46, 47]

In this study, we designed several BsAbs based on 3 basic design formats for active targeting of the EnGeneIC delivery vehicle (EDV^{TM}nanocell) to the epidermal growth factor receptor (EGFR), to replace the currently used protein A/G linked mAbs.[48-50] The EDV^{TM}nanocell (a 400 nm particle of bacterial origin capable of carrying a drug payload) was originally targeted using a BsAb moiety produced by incubating 2 different mAbs with protein A/G (Pierce, USA).[21] Although functional BsAbs capable of delivering the EDV^{TM}nanocell were prepared, it was noted that multimer formation and the inability to control the ratio of mAbs bound to the protein A/G, which has 6 potential Fc-binding sites, rendered the targeting entity unsuitable for commercial manufacture and downstream clinical trials.[21, 32] Recombinant BsAbs offer an advantage of producing one antibody with dual target binding capability.

The EDV^{TM}nanocell is coated with lipopolysaccharide (LPS),[21] and thus BsAb designs incorporated scFvs derived from an anti-LPS antibody (1H10) with the anti-EGFR antibody ABX-EGF.[51-53] ABX-EGF (panitumumab) was developed via transgenic humanized mouse technology by Abgenix Inc.,[51-53] and is approved for clinical use in the treatment of colorectal cancer. ABX-EGF has picomolar affinity for EGFR, and its properties, including affinity, specificity and immunogenicity, have been extensively evaluated and is an ideal model antibody to incorporate into the design and testing of bispecific formats.[21] Three BsAb formats were evaluated for EDV^{TM}nanocell targeting; a G4S-linked tandem scFv format, homodimeric Fc-containing BsAbs and KIH-engineered formats to promote forced heterodimerisation of the EDV-targeting variable fragments.

Table 1. BsAb format and sequence design parameters. (**A**) Tandem scFv, (**B**) Fc-containing and (**C**) Knobs-into-Holes (KIH) BsAbs. (**A**) The tandem scFv, incorporated a G4S linker as well as N-terminal His and C-terminal myc tags. Homodimeric Fc-containing variants (**B**) incorporated an IgG1-Fc linker; variants of (**B**) included either G4S or a longer (***Longlink***) linker to connect 1H10 scFvs to the CH3 domain. Variants also included or excluded engineered cysteine residues in scFvs for enhanced stability. KIH constructs (**C**) are heterodimers with 1H10 heavy and light variable regions on separate chains. Format design included a longer (***Longlink***) linker connecting CH3 to 1H10 variable fragments and again either included or excluded engineered cysteine residues in scFvs

	BsAb ID	Sequence information	Additional disulfide bridges	CH3-αEDV Linker		Structural Illustration
				G4S	Longlink	
A	Tandem scFv	His-(ABX-EGF scFv)-*G4S*-(1H10 scFv)-myc	✗	NA	NA	
B	Fc-containing	(ABX-EGF scFv)-*G4S*-Fc-*G4S*-(1H10 scFv)	✗	✓	✗	
	Fc-containing (Longlink)	(ABX-EGF scFv)-*G4S*-Fc-*Longlink*-(1H10 scFv)	✗	✗	✓	
	Fc-containing (Cys)	(ABX-EGF scFv) (cys)-*G4S*-Fc-*G4S*-(1H10 scFv) (cys)	✓	✓	✗	
	Fc-containing (Cys Longlink)	(ABX-EGF scFv) (cys)-*G4S*-Fc-*Longlink*-(1H10 scFv) (cys)	✓	✗	✓	
C	KIH 1 (Cys)	(ABX-EGF scFv) (cys)-*G4S*-Fc(Knob)-*Longlink*-VH(1H10)(cys) + (ABX-EGF scFv) (cys)-*G4S*-Fc(Hole)-*Longlink*-VL(1H10)(cys)	✓	✗	✓	
	KIH 2	(ABX-EGF scFv)-*G4S*-Fc(Knob)-*Longlink*-VH (1H10) + (ABX-EGF scFv)-*G4S*-Fc(Hole)-*Longlink*-VL (1H10)	✗	✗	✓	

Additionally, modifications of the latter 2 formats were investigated, incorporating additional disulfide bridges in the scFv domains and longer linkers between the Fc-CH3 and anti-LPS scFv interface (Table 1). We evaluated these different formats with regard to expression yields, their ability to bind respective targets and their effect on EDV^{TM}nanocell clumping. The tandem scFv design was further evaluated to show its ability to target the EDV^{TM}nanocell to MDA-MB-468 breast cancer cells overexpressing EGFR in vitro, and to target the drug-loaded EDV^{TM}nanocell to mouse xenografts in vivo, resulting in tumor regression.

Results

Production and yield

Various BsAbs of different designs were expressed in Chinese hamster ovary (CHO)-S transient cell culture and purified from culture supernatant. We observed that BsAb yields from transient CHO-S cultures were lower compared to that of full length, ABX-EGF-IgG1 mAb (52.6 mg/L); tandem scFv BsAb expression routinely yielded around 5 mg/L in transient cell culture supernatant, whereas yields of Fc-containing and KIH BsAbs increased 2-3 fold compared to that of the tandem scFv BsAb. Engineering disulfide bridges into Fc-containing and KIH variant scFvs dramatically decreased BsAb yields 6-9 fold compared to those of non-stabilised formats. A qualitative Western blot confirmed that BsAbs were efficiently secreted and that the lower product yields were not due to retention in the endoplasmic reticulum via cellular mechanisms such as the unfolded protein response (results not shown). [54-57]

Targeted binding

Binding activity was maintained for both EGFR and LPS targets for all engineered BsAb formats (Table 2; **Fig. 2**). Surface plasmon resonance (SPR) analysis of recombinant EGFR binding using Biacore T-200 (GE) showed that BsAb association constants (k_a) were 5 to 10-fold lower than that of the published ABX-EGF (using purified native EGFR).[58, 59] Dissociation constants (k_d) of the ABX-EGF-scFvs incorporated within the tandem scFv, Fc-containing and Fc-containing (Longlink) BsAbs have values similar to the published k_d for ABX-EGF-IgG2 mAb, whereas all remaining EGFR-targeting formats have k_d values up to 10-fold slower. A control, non-specific tandem scFv BsAb targeting RSV and LPS, showed no binding to EGFR.

Table 2. Surface plasmon resonance binding affinities for recombinant EGFR-mFc collected from a Biacore T-200. Surface Plasmon Resonance (Biacore) analysis of BsAb binding to EGFR – k_a (association constant), k_d (dissociation constant), and K_D (binding affinity). High performance (Multi-cycle) Kinetic Assay (HPKA) data is shown for all BsAb constructs as well as for a reassembled, complete IgG1 ABX-EGF mAb. Standard error values corresponding to binding values of recombinant EGFR is shown as $\pm$ x $\times$ 10^6 for k_a and $\pm$ y $\times$ 10^{-5} for k_d

	Binding to recombinant EGFR		
Antibody ID	**k_a (1/Ms) ($\times 10^6$) ($\pm$SE)**	**k_d (1/s) ($\times 10^{-5}$) ($\pm$SE)**	**K_D (nM)**
ABX-EGF IgG2 mAb (published)	1.97	11.3	0.05
ABX-EGF IgG1 mAb (reformatted)	2.18 $\pm$ 0.0025	15.5 $\pm$ 0.047	0.07
Non-specific Tandem scFv	No binding	No binding	No binding
Tandem scFv	0.26 $\pm$ 0.0004	13.6 $\pm$ 0.021	0.52
Fc-containing	0.36 $\pm$ 0.0023	9.42 $\pm$ 0.028	0.26
Fc-containing (Longlink)	0.19 $\pm$ 0.0005	21.6 $\pm$ 0.084	1.13
Fc-containing (Cys)	0.48 $\pm$ 0.0002	4.89 $\pm$ 0.019	0.10
Fc-containing (Cys Longlink)	0.70 $\pm$ 0.0004	2.47 $\pm$ 0.025	0.04
KIH 1 (Cys)	0.82 $\pm$ 0.0005	2.67 $\pm$ 0.026	0.03
KIH 2	0.50 $\pm$ 0.0021	6.75 $\pm$ 0.021	0.13

Reformatting the ABX-EGF-scFv to an IgG1 mAb resulted in similar k_a, k_d and binding affinity (K_D) values as those reported for the published ABX-EGF IgG2 mAb (**Fig. 2**). K_D for the EGFR-targeting BsAbs were all in the nanomolar (nM) range.

The Fc-containing (Longlink) BsAb showed a 4 to 5-fold decrease in K_D compared to that of the Fc-containing BsAb. Flexibility imparted by the long linker may have a destabilizing effect on the scFvs within the BsAb. Interestingly, cysteine stabilization restores the high affinity of Fc-containing (Longlink) BsAb for EGFR (0.04 nM). Similarly, cysteine-stabilised KIH 1 (Cys) BsAb showed greater binding affinity than that of the KIH 2 BsAb. Although the reasons for the effect of cysteine stabilization of scFvs within a specific BsAb format were not investigated, it is hypothesized that the additional disulfide bonds offer a further degree of stabilization and rigidity within the scFv binding entities, which enhances binding affinity.

Binding of all BsAbs to LPS was confirmed by ELISA (results not shown). As LPS is naturally adhesive and binds strongly to surfaces (e.g., glass, plastic), performing binding studies by SPR was not compatible with the microfluidics system of the Biacore. The kinetics of 1H10-scFv component of the BsAbs binding to LPS were therefore determined by the Octet system (ForteBio), which circumvents the problems of a fluidics-based system, and provided binding data for the original, hybridoma-derived 1H10-mAb [K_D = 0.2 nM, k_a = 8.20E+05 ($\pm$1 .25E+04), k_d = 1.36E-04 ($\pm$1 .72E-05)] and 1H10-scFv of the tandem scFv format [K_D = 10.0 nM, k_a = 2.20E+04 ($\pm$1 .76E+03), k_d = 5.64E-04 ($\pm$2.39E-05)] (**Fig. 2C**). The 60-fold difference in K_D between the 2 formats is indicative of differences in avidity.

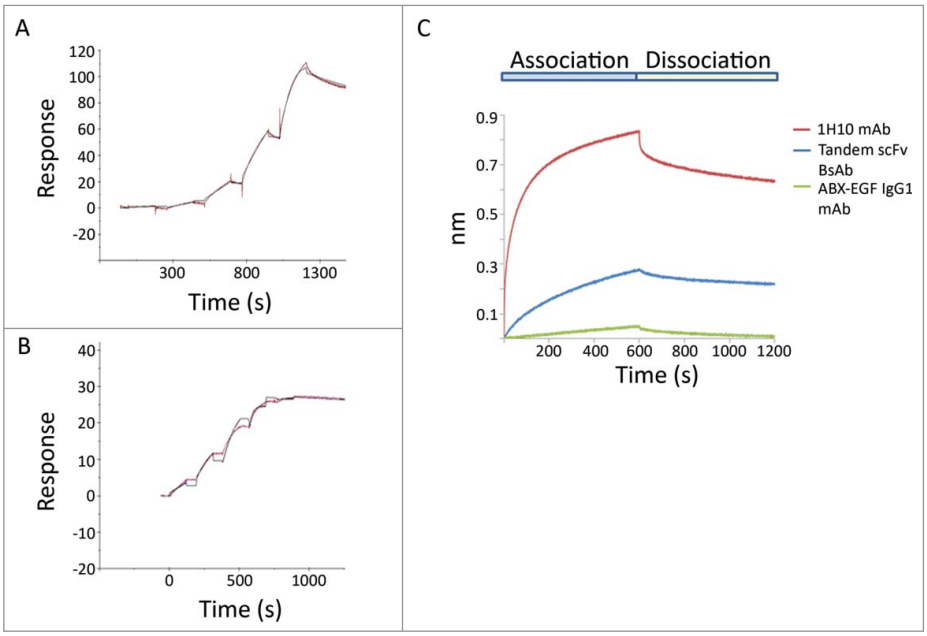

Figure 2. ABX-EGF and 1H10 representative binding curves. SPR sensorgrams illustrative of (**A**) ABX-EGF tandem scFv (1 nM, 3 nM, 10 nM, 30 nM and 100 nM BsAb) and (**B**) ABX-EGF-IgG1 mAb (1 nM, 3 nM, 10 nM and 30 nM BsAb) binding to immobilised recombinant EGFR. (**C**) Biolayer interferometry kinetic curve of ABX-EGF tandem scFv the 1H10-mAb and ABX-EGF IgG1 mAb at 100 nM binding to captured LPS.

Flow cytometry analyses showed that all EGFR-targeting formats (mAb and BsAb) were able to bind to EGFR-over-expressing MDA-MB-468 cells, while non-specific formats showed no binding (**Fig. 3A-C**). A decreased shift for the tandem scFv BsAb compared to the Fc-linked formats can be attributed to the higher avidity of the EGFR-bivalent, Fc-linked BsAbs. The lower fluorescence intensity of the tandem scFv could also be due to the different secondary antibody used for detection.

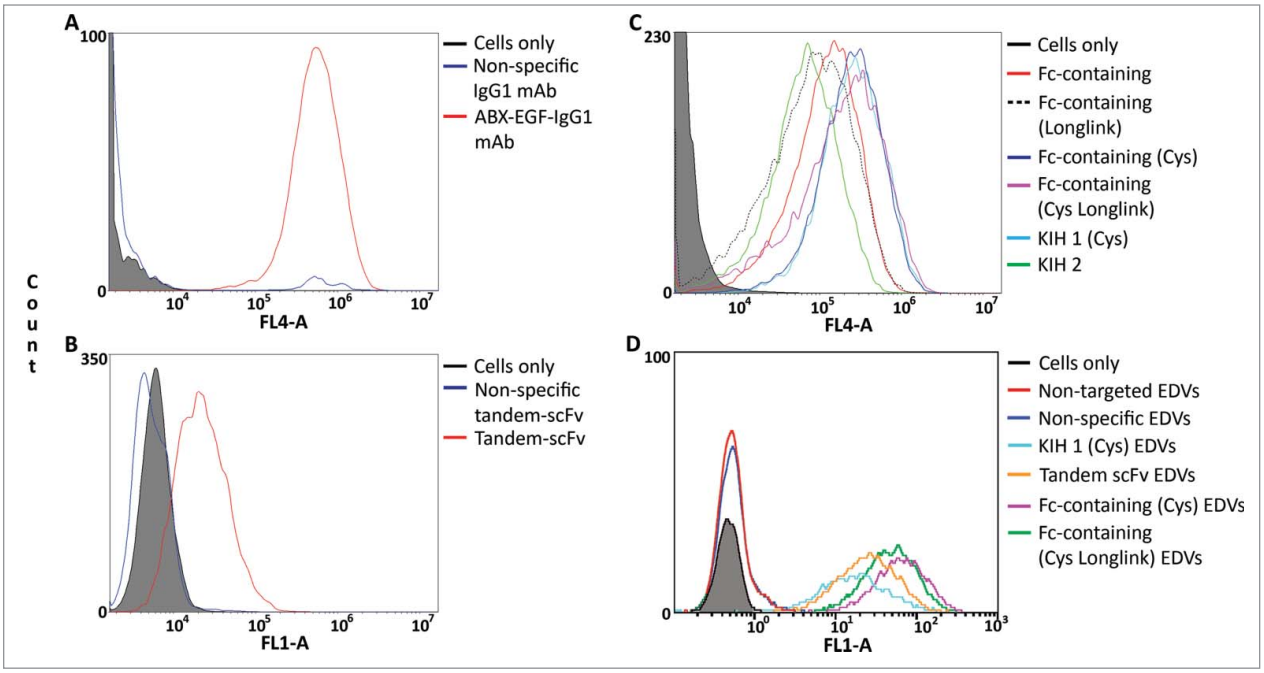

Figure 3. In vitro binding of IgG1 mAbs, BsAbs and BsAb-EDVs to EGFR overexpressing MDA-MB-468 breast cancer cells. All specific BsAbs include ABX-EGF-scFvs (anti-EGFR), non-specific formats include a palivizumab-scFv (anti-RSV) and all BsAbs include the 1H10 (anti-LPS) scFv. (**A**) Whole mAbs, non-specific (anti-RSV) and ABX-EGF-IgG1 (anti-EGFR) binding to cells detected by APC-conjugated anti-human IgG; (**B**) Tandem scFv BsAbs (anti-RSV and anti-EGFR) binding to cells detected by FITC-conjugated anti-c-myc; (**C**) Various Fc-containing BsAbs binding to cells detected by APC-conjugated anti-human IgG; and (**D**) AlexaFluor 488 labeled EDV^{TM}nanocells (EDVs) binding to cells via various bound BsAbs.

It was of interest to investigate the ability of BsAbs to crosslink the 2 antigens LPS and EGFR. A co-localization experiment using fluorescently labeled recombinant-EGFR (DL650) and BsAb-targeted EDV^{TM}nanocells (AF488) provided visual confirmation that BsAbs could simultaneously bind their 2 targets (**Fig.** 4). Results show that non-targeted and non-specifically targeted EDV^{TM}nanocells do not co-localize in the presence of recombinant EGFR (green fluorescence only). We included all 7 of the BsAb formats, and observed their effect on nanocell clumping. The ABX-EGF tandem scFv, KIH 1 (Cys), Fc-containing (Cys) and Fc-containing (CysLonglink) BsAbs caused less EDV^{TM}nanocell aggregation, as illustrated by a uniform distribution of co-localized EGFR and targeted EDV^{TM}nanocells, whereas nanocells targeted with KIH 2, Fc-containing and Fc-containing (Longlink) BsAbs produced large, aggregated clumps of co-localized recombinant EGFR and EDV^{TM}nanocells. This illustrates how different recombinant BsAbs affect the EDV^{TM}-nanocells during and post targeting, and the final product stability. These findings highlight how BsAb design and properties in solution may influence the performance of the BsAb-EDV^{TM}nanocell formulated product.

The BsAbs that resulted in a uniform distribution in the co-localization study were further investigated by binding to cells using flow cytometry (**Fig. 3D**) and confocal microscopy (**Fig. 5**). For confocal microscopy, MDA-MB-468 cells (labeled with AF647) were targeted with AF488-labeled BsAb-EDVs. Non-targeted EDV^{TM}nanocells did not localize on MDA-MB-468 cell surfaces nor did non-specific EDV^{TM}nanocells. Confocal microscopy (**Fig. 5**) and flow cytometry analyses (**Fig. 3D**) showed that while all BsAbs localized on the MDA-MB-468 cell surface, the tandem scFv and KIH 1 (Cys) BsAb formats, possessing only one 1H10-scFv, displayed a lower distribution across the cell surface compared to the distributions of the Fc-containing (Cys) and Fc-containing (CysLonglink) targeted EDV^{TM}nanocells, with 2 1H10-scFvs.

Stability

Various buffer formulations were tested to improve the storage stability of the BsAbs. Formulations tested thus far have not shown significantly improved stability of Fc-containing and KIH variants, and there is evidence of concentration-dependent aggregation above 0.1 mg/ml (results not shown). Size exclusion chromatography (SEC) HPLC analyses over a 1 month period indicated that tandem scFv stability, when stored at a concentration of 0.12 mg/ml, is affected by buffer formulation. Product storage in a formulation of PBS/trehalose resulted in slightly increased aggregation levels when stored at -20°C compared with 4°C. However, stability was maintained at both 4°C and -20°C in a HEPES/Trehalose buffer formulation (**Fig. 6A**). Dynamic light scattering (DLS) data confirmed the tandem scFv to be a monomer of 55 kDa in size, with a hydrodynamic radius of 2.5 nm (results not shown). Thermostability determined by

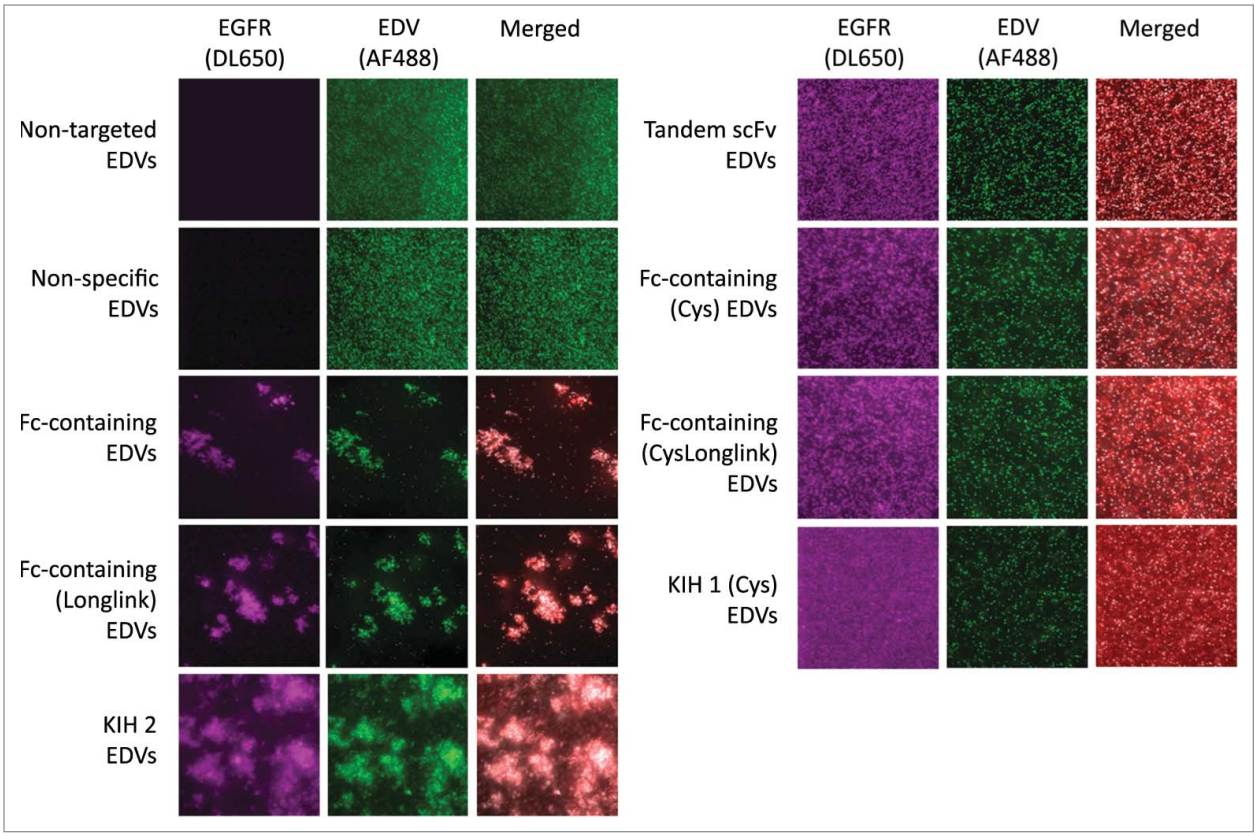

Figure 4. Co-localization imaging by confocal microscopy of recombinant EGFR-His (DL650) and EDV^{TM}nanocells (AF488) with or without specific BsAb. Recombinant EGFR was co-incubated with EnGeneIC Delivery Vehicles (EDV^{TM}nanocells or EDVs) pre-targeted with various BsAbs prior to microscopy. EDV^{TM}nanocells are represented in green (AF488) while DyLight650-labeled EGFR-His is represented in purple (color substitution from red has been applied to improve co-localization imaging). Overlap of the 2 fluorophores (co-localization) results in near-white imaging. Panels represent the filter showing EGFR (DL650) alone, EDV (AF488) alone and the merged overlay image of the 2.

differential scanning calorimetry (DSC) indicated that the tandem scFv has a melting temperature (Tm) of 57°C (**Fig. 6B**). Additionally, co-incubating the tandem scFv with human serum (HS) over a 48-hour period showed no protease-mediated degradation of the BsAb (results not shown).

EDV^{TM}nanocell-mediated tumor regression in a mouse xenograft model

Due to the superior properties of the tandem scFv BsAb, it was the only recombinant BsAb format tested in a mouse xenograft model for tumor regression. To evaluate the efficacy of EDV^{TM}nanocells targeted using the ABX-EGF tandem scFv ($^{Tandem\ scFv}$ EDV) compared to those targeted with EnGeneIC's original, Protein A cross-linked anti-LPS / anti-EGFR BsAb ($^{Protein\ A/G}$ EDV),[21] in vivo experiments were carried out utilizing a MDA-MB-468 mouse xenograft model, with dosing commencing 14 d after subcutaneous injection of MDA-MB-468 cells (tumor volume approx. 80–100 mm^3) (**Fig. 7**). EDV^{TM}nanocells targeted with the tandem scFv and loaded with doxorubicin ($^{Tandem\ scFv}$ EDV $_{Dox}$) effectively suppressed tumor growth over a 38 day period post xenograft compared to controls. Active targeting with $^{Tandem\ scFv}$ EDV $_{Dox}$ showed tumor regression was similar to that achieved with EDV^{TM}nanocells targeted by protein A/G cross-linked BsAbs ($^{Protein\ A/G}$ EDV $_{Dox}$). Importantly, active targeting of doxorubicin-loaded EDV^{TM}nanocells by the tandem scFv BsAb resulted in a 40% reduction in tumor volume compared to that of loaded passively targeted EDV^{TM}nanocells (EDV $_{Dox}$) 38 d post xenograft (i.e., 140 mm^3 and 240 mm^3, respectively). Targeted EDV^{TM}nanocells not loaded with doxorubicin ($^{Tandem\ scFv}$ EDV) had a minor tumor suppressing effect, whereas non-targeted, doxorubicin-loaded EDV^{TM}nanocells (EDV $_{Dox}$) showed significant tumor regression compared to saline controls; the latter being most likely due to passive targeting through leaky tumor vasculature of tumor xenografts (pore sizes 0.2–1.2 μm).[32,60,61]

Discussion

A variety of BsAb formats were investigated for their ability to bind EDV^{TM}nanocells and recombinant or native EGFR. This initial proof-of-principle study was performed using BsAbs containing the scFv binding sequence derived from ABX-EGF (panitumumab), a rigorously tested, approved therapeutic antibody, which has ideal properties such as high affinity and stability. ABX-EGF targets EGFR, which is commonly over-expressed on

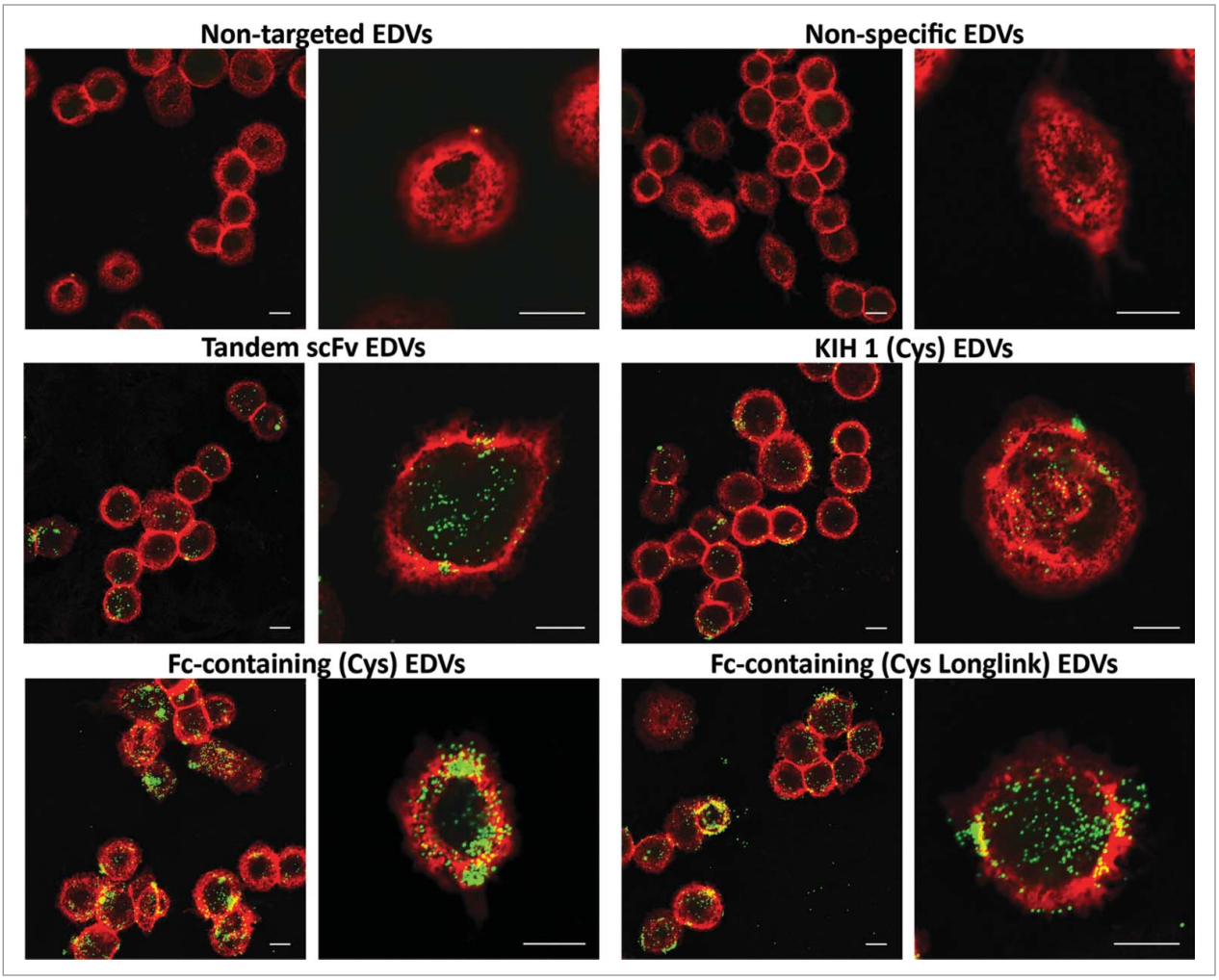

Figure 5. Confocal in vitro imaging of stable BsAb-EDV™nanocells binding to the surface of MDA-MB-468 breast cancer cells. MDA-MB-468 cells were labeled with anti-EGFR-AF647 (red) to visualize the cell surface while BsAb-EDVs were labeled with AF488 (green). After 3 hours of incubating labeled BsAb-EDVs with EGFR overexpressing MDA-MB-468 cells, the samples were washed, fixed and labeled with the AF647. Cover slips were mounted and cells visualised on a Confocal LSM Zeiss 710 using a Plan-Apochromat 63x/1.40 Oil DIC M27 objective. Analyses were performed using ZEN 2008 software. Scale bars in white indicate a length of 10 μm.

a variety of cancer cells and the target for several marketed anti-cancer therapeutics.[3,7,50,62] The modular nature of BsAb constructs allows alternative antibody specificities to be substituted depending on the receptor target.

The tandem scFv BsAb was designed to include a 5 amino acid glycine-serine linker (G4S) between the ABX-EGF- and 1H10-scFv. The shorter linker reduces flexibility and therefore prevents misfolding from occurring between the 2 scFv components. Administered in isolation, tandem scFv BsAbs exhibit low avidity and, due to their small size, a low serum half-life;[46, 47] however, pharmacokinetic properties of tandem scFv BsAbs bound to the large EDV™nanocell (400 nm in diameter) will be enhanced. Furthermore, coating of the EDV™nanocell with tandem scFv BsAbs imparts multivalency and avidity to the NP, and provides multiple binding sites for the cancer-targeting domain.[21]

To produce more complex BsAbs compared to the tandem scFv BsAb, manipulation of the standard IgG mAb format has produced a plethora of Fc-containing BsAbs, whereby designs generally rely on the principle that Fc-containing BsAbs will dimerize through the Fc, similar to native, whole mAbs.[11,46,47,63,64] Features of these antibodies include engineering Fc components to improve or remove various related functions, forced heterodimerisation, removal of redundant domains and addition of other binding motifs to the IgG molecule.[47,63,65-67] We used an IgG1 Fc-domain to link and separate the 2 scFvs spatially (ABX-EGF scFv at the N-terminus of human IgG1 Fc domain, and an 1H10 scFv at the C-terminus) to create the ABX-EGF-Fc-1H10 homodimeric Fc-containing BsAb, similar to the scFv-Fc-scFv BsAb dimer described in Jendreyko *et al.* and the Emergent Biosolutions™ product termed ADAPTIR™ Multi-Specific.[68, 69] A benefit of the Fc-containing

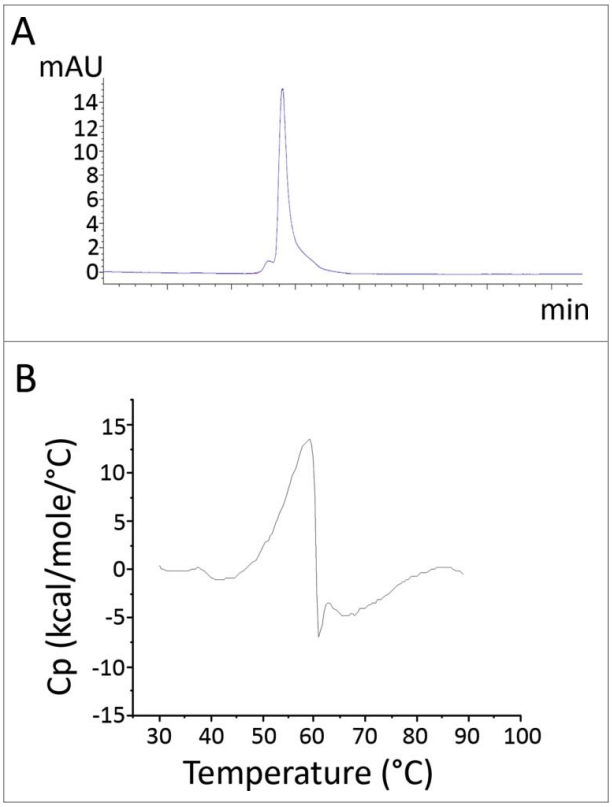

Figure 6. Tandem scFv stability data. (**A**) Tandem scFv samples were stored in various buffers at different temperatures to evaluate stability during storage over a 3 month period. The representative trace is indicative of stable product stored in Hepes/trehalose buffer for 3 months. (**B**) Thermostability of tandem scFv BsAb in PBS was determined by differential scanning calorimetry and indicates unfolding and subsequent aggregation of the tandem scFv BsAb at 57°C.

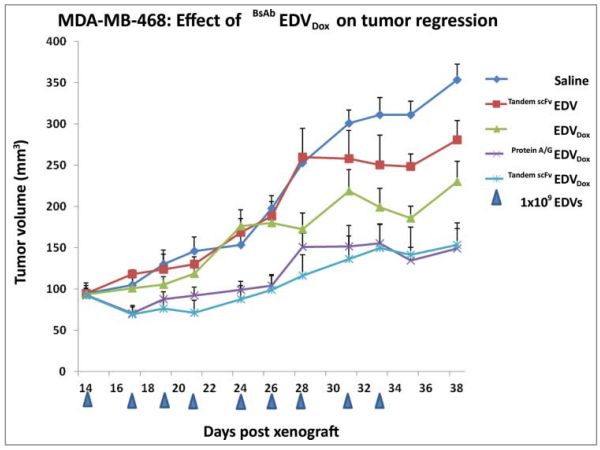

Figure 7. Mouse MDA-MB-468 xenograft results following EDV^{TM}nanocell (EDV) treatment. Tandem scFv refers to the EGFR targeting ABX-EGF BsAb format in the BsAb-EDV^{TM}nanocell configuration whereas protein A/G refers to EnGeneIC's original BsAb format composed of anti-EGFR and 1H10 mAbs connected through a protein A/G molecule. Dox refers to the chemotherapeutic agent doxorubicin. At various time points, indicated with a blue triangle, mice were treated with 1×10^9 EDVs.

BsAbs over the tandem scFv format is the presence of 2 scFvs to bind each target – promoting high avidity binding to both the EDV^{TM}nanocell and the EGFR on the cancer cell surface; whereas a potential drawback could result if the Fc-domain stimulates an unwanted immune response and complement cascade.[20,31] Although it is well known that Fc-related immune responses can be avoided through various mutations [67] throughout the domain, our work thus far has focused on the production of a stable drug delivery system rather than on potential immunogenicity. EnGeneIC's original BsAb format also retained fully functional Fc domains without significant immunogenicity being noted.[21,22,31]

Previous studies have found that inclusion of a number of design modifications, including variations in CH3-scFv linker length and type, and also scFv stability engineering via addition of disulfide bonds, improved construct stability. [70-75] A concern with the Fc-linked dimeric design was whether the presence of 2 anti-LPS scFvs would result in EDV^{TM}nanocell aggregation via binding of multiple nanocells rather than high avidity binding of a single nanocell. An alternative Fc-linked BsAb was engineered consisting of 2 EGFR targeting scFvs at the N-terminus (high avidity) and a single anti-LPS scFv at the C-terminus of the final product. Heterodimeric BsAb formats were based on the common KIH constructs[65, 75] and partly on the TandAb BsAb designed by Affimed where variable linker lengths are used to determine chain association for functional BsAb formation.[76, 77] The single anti-LPS site is formed through forced heterodimerisation of the CH3 domain via KIH engineering, where the V_H and V_K domains of the scFv are expressed on separate polypeptides in a single cell. To ensure that the V_H- and V_K-chains associate with one another to form a functional 1H10-scFv, a longer linker between CH3 and the 1H10-scFv component was designed to allow extra flexibility in the area for functional association of the nanocell-targeting scFv components.[75]

Based on co-localization images of the various BsAb formats binding to EDV^{TM}nanocells and to EGFR, 4 of the BsAbs are of particular interest for further development: tandem scFv, Fc-containing (Cys), Fc-containing (Cys Longlink) and KIH (Cys). The other formats resulted in clumping of the EDVs. However, as the expression yields of the disulfide-engineered, Fc-linked BsAbs were 6-9 fold lower than the tandem scFv, the tandem scFv was chosen for further investigation.

Tumor regression in MDA-MB-468 breast cancer cell xenografts showed that BsAb-mediated targeting with anti-EGFR antibody is essential for optimal inhibition of tumor growth. Although EDV^{TM}nanocells have previously been successfully targeted by cross-linking 2 IgG antibodies with protein A, utilizing the tandem scFv, whereby one arm binds the EDV^{TM}nanocell and the other targets the tumor, requires the production of a new molecular entity (NME). A biologic NME can be characterized for binding activity and manufactured according to cGMP. The coating of BsAb on the surface of the EDV^{TM}nanocell also imparts other properties to the nanocell. Depending on BsAb density on the nanocell surface, the imparted avidity would enhance apparent affinity of the EDV^{TM}nanocell for its target, compared to that of the target scFv alone. Furthermore, coating

with a BsAb, where the targeting scFvs are of human origin, alters the physicochemical properties of the EDV^{TM}nanocell in vivo, and would affect parameters such as pharmacokinetics and immunogenicity.

Nanomedicine is poised to play an increasingly important role in cancer therapy in the future, with at present 7 passively targeted nanomedicines approved for cancer therapy.[32, 33] Actively targeting nanoparticles to tumors with antibodies, as demonstrated in this study, can have significant advantages and improve efficacy compared to passive targeting alone. Designing new BsAbs that are able to efficiently target nanoparticles opens a new dimension in active nanoparticle targeting.

Materials and Methods

Sequence design

The DNA sequence of the extracellular domain (amino acid residues 25 - 645) of wild type human EGFR (Swiss-Prot P00533) was synthesized by Geneart, incorporating a mammalian leader sequence from IgK and a C-terminal His tag, with codon optimisation for expression in CHO cells. Further constructs consisting of amino acid residues 25 - 525 followed by either human or mouse Fc tags were created, similar to that described by Adams, 2009.[78] The heavy and light chain variable region sequences of the anti-LPS monoclonal antibody were determined by isolating and sequencing cDNA isolated from the hybridoma 1H10, using established protocols.[79] The sequence information for the heavy and light chain variable regions for panitumumab (ABX-EGF) was obtained from US Patent 6 235 883. The sequence for an unrelated control antibody (anti-RSV) palivizumab (Synagis®), was obtained from the RCSB Protein Data Bank file, 2 HWZ.

The DNA templates for all BsAb formats were synthesized by Geneart with codon optimisation for CHO expression, then cloned into the mammalian expression vector pcDNA3.1 (Invitrogen). Cysteine stabilization substitutions were made at Kabat position VH44 and VL100 of the scFvs.[72, 73] Variants included either a short (G4S) linker or a longer linker (SSDKTHTSPPSPGGGGSGGGGSGGGGSGGGG), as described in Moore *et al.*, connecting the CH3 domain to the 1H10-scFv.[75] A "knob" was produced by amino acid substitution for a longer side chain (T366'W), whereas a "hole" was produced by amino acid substitutions for shorter side chains (T366'S:L368'A:Y407'V); the sequence positions are as indicated by Kabat *et al.*[80] The tandem scFv included 6xHis and c-myc tags for purification and detection, while the other constructs utilised the Fc domain for purification and detection. For the KIH constructs, 2 DNA templates were required, one containing the 1H10 Vh region and one containing the 1H10 Vk region. Whole mAbs for panitumumab (ABX-EGF) and palivizumab were created by reformatting the BsAb sequences using a previously described method.[81]

Mammalian expression and purification

Transient expression of all BsAbs was performed using PEI-mediated transfection of suspension adapted CHO cells as previously described.[82] KIH chains were co-transfected at a 1:1 DNA ratio (1H10-Vh : 1H10-Vk). Culture supernatants were harvested 7 - 10 d post-transfection by centrifugation, then filtered and stored frozen at -80°C until purification could be completed.

For the tandem scFv purification, 2 sequential IMAC chromatography steps were utilised, first with HisTrap Excel (GE Healthcare), which tolerates nickel-chelating agents present in mammalian cell culture media, followed by HisTrap FF (GE Healthcare), which further removes impurities. Manufacturer-recommended buffers were used for equilibration and loading, with 500 mM Imidazole added for elution. The eluted product was buffer exchanged into PBS using a HiPrep desalting column after each IMAC step. Tandem scFv BsAb monomer was isolated using a GE gel filtration column (HiPrep 26/60 Sephacryl S-200 HR) and the monomer subsequently used for kinetic experiments and long-term stability studies.

For constructs containing an Fc domain, purification was performed in one step using a MabSelect Sure Protein A HP column. Following purification the BsAbs were desalted using the HiPrep desalting column into Dulbecco's PBS buffer for storage at 4°C unless specified otherwise.

Dynamic Light Scattering

Analysis was completed by CSL, Melbourne, Australia. Molar mass and hydrodynamic radius (Rh) was determined using SEC-MALS. A Wyatt WTC-030-N5 4.6 column was used with buffer composed of 100 mM phosphate/200 mM sodium chloride, pH 6.8. The column was equilibrated in the buffer and flow rate set to 0.2 ml/min with 100 μl sample injections. A DAWN Heleos MALS detector was normalized using BSA and used in series with an Agilent 1200 series UV diode array detector and an Optilab T-rEx RI detector. Wyatt's Astra VI software was used to calculate the weight-averaged molar mass and hydrodynamic radius.

Analysis of tandem scFv by differential scanning calorimetry

The tandem scFv BsAb was concentrated to 1 mg/ml in PBS using membrane based centrifugal concentrators with nominal molecular weight cutoff of 10 Kda (Millipore). 500 μl of 1 mg/ml tandem scFv was vacuum degassed and loaded into the sample chamber of the VP differential scanning calorimeter (VP-DSC, Microcal). The same volume of PBS was loaded into the reference chamber. The sample and reference chambers were scanned once from 25°C to 90°C for 1 h to determine the melting profile of the tandem scFv. The data was analyzed using Origin 7.0 software and graphed as time (min) (x axis) versus heat capacity (Cp) (y axis).

Size exclusion chromatography HPLC

A mobile phase of 0.1 M sodium phosphate buffer, 0.2 M sodium chloride, pH 6.8 was prepared and filtered using a 0.22 μm filter. A gel filtration standard was included on each run of the HPLC to calculate molecular weights by their retention times. Samples were not concentrated prior to performing

SEC so as to avoid the potential that concentration-based aggregation may occur. The guard column and SEC-HPLC column were connected to the HPLC system, flushed and equilibrated in mobile phase. 100 μl sample injections were used in all cases with a flow rate of 0.8 ml/min. Columns were stored in 20% ethanol pre- and post-run completion.

Tandem scFv stability in buffer formulations of PBS/trehalose and HEPES/trehalose was completed by The Australian Protein Analysis Facility. SEC was performed using a Zorbax BioSeries GF-250 column (Agilent). Flow rate was set to 0.5 ml/min and a mobile phase of 100 mM sodium phosphate, pH 7, 250 mM NaCl used as a buffer. Sample injections were set to 25 μl.

Surface plasmon resonance

To evaluate binding affinities of the EGFR-targeting ABX-EGF-scFvs on all constructs, kinetic data was collected from either Single Cycle Kinetic (SCK) Assays or High Performance (Multi-cycle) Kinetic Assays (HPKA) performed on a Biacore T-200. A CM5 chip was coated with an anti-mouse IgG antibody on flow cells 1 and 2 as described in the Mouse Antibody Capture Kit guidelines (GE Healthcare). Recombinant EGFR-mFc was captured on flow cell 2 at 10 μg/ml for 8 - 15 seconds and variable concentrations of BsAb (1 – 100 nM) flowed over both flow cells 1 and 2. Recommended flow rates (30 μL/min) and regeneration conditions (10 mM glycine pH 1.7; 10 μL/min for 180 s) were used. The dissociation phase was 1800 s. Reference subtractions of flow cells 2 - 1 were incorporated in the analysis as were blank and buffer only sample runs. Kinetic analyses were performed using a 1:1 fit of binding curves using BiaEvaluation software (GE Healthcare).

Biolayer interferometry kinetic characterization of LPS binding

The binding of mAbs and BsAbs to LPS molecules was tested utilizing Biolayer Interferometry and the ForteBio Octet module. Aminopropylsilane (APS) biosensors (ForteBio) were briefly hydrated in PBS and coated with 1 mg/ml LPS (*Salmonella enterica*, serotype *typhimurium* - Sigma L7261) diluted in PBS. A concentration range of the 1H10-mAb (anti-LPS) or tandem scFv BsAb was set up using 2-fold dilutions starting at 100 nM and subsequently tested for binding to immobilised LPS. PBS was added to LPS coated sensors as a reference.

Flow cytometry of BsAb and mAb samples against MDA-MB-468 cells

All BsAb and mAb samples had been stored at 4°C prior to commencement of the experiment. The Indirect Flow Cytometry (FACS) Protocol described by Abcam was used (available online at http:\\www.abcam.com). All components were added to a cell suspension of 2×10^5 MDA-MB-468 cells in 100 μl of 10% FCS/DPBS and kept at 4°C to prevent receptor-mediated endocytosis from occurring. Primary BsAb and mAb stock dilutions to 10 μg/ml were made in ice cold 5% BSA + Dulbecco's PBS buffer as were secondary antibody dilutions. Final BsAb and mAb concentrations were at 1 μg/ml in the final cell suspension volume. Mouse anti-c-myc:FITC (AbD Serotec; Bio-Rad) was used as the secondary antibody for detecting binding shifts when the ABX-EGF tandem scFv and non-specific tandem scFv were incubated with MDA-MB-468 breast cancer cells; whereas APC-conjugated $F(ab)'_2$ fragment goat anti-human IgG (Jackson ImmunoResearch) was used for detection of all mAb, Fc-containing and KIH constructs. Fluorescence shift was then analyzed on the Accuri C6 flow cytometer. Cells were gated using forward and side scatter, and the cell sample incubated with secondary antibody only was used to determine the cut-off fluorescence for non-specific binding. Events were limited to 100 μl or 100,000 events.

Preparation of labeled BsAb-EDV^{TM}nanocells

One $\times 10^{12}$ Non-targeted EDV^{TM}nanocells were incubated with 1 mg of Invitrogen's NH2-reactive AlexaFluor488 (internal protocol) and excess dye was removed by 4 spin wash cycles in sterile PBS. The fluorescently labeled EDV^{TM}nanocells were counted using a Nanocyte and found to be 5×10^{10} EDVs/ml at EnGeneIC Pty Ltd. Doses were prepared as 2.5×10^{10} EDV (AF488) particles in 0.5 ml. 2.5×10^{10} EDV (AF488) particles were incubated with 6 μg of various BsAb constructs at room temperature for 30 min while shaking at 300 rpm. Samples then underwent 3 PBS spin wash cycles at 9,000 g for 8 min each to remove any excess BsAb. BsAb-EDV^{TM}nanocells were resuspended to concentrations as required for specific experiments.

Flow cytometry analysis of EDV^{TM}nanocell binding to MDA-MB-468 cells

One $\times 10^5$ MDA-MB-468 cells grown on coverslips in 400 μl RPMI + 5% FCS + 1% PC-SM were treated with 1×10^9 pre-targeted and AF488-labeled EDV^{TM}nanocells and returned to 37°C for 3 h. This was repeated for the non-targeted EDV^{TM}nanocell and each of the 5 BsAb-EDV^{TM}nanocells – non-specific and ABX-EGF tandem-scFv, KIH 1 (Cys), Fc-containing (Cys) and Fc-containing (CysLonglink), with only the control remaining untreated. On completion of the 3 h incubation period, coverslips were washed 3 times with sterile DPBS and cells scraped for flow analyses on a Beckman FC500 flow cytometer. Flow rate was set to high and cells were again gated using forward and side scatter. The "cells only" sample was used to determine the cut-off fluorescence for non-specific binding. Events were detected over a 250 sec period. Final analyses were completed using CXP and VenturiOne software.

Co-localization

AF488-Labeled, non-targeted and targeted EDV^{TM}nanocells were prepared as previously mentioned and observations made regarding clumping of the BsAb-EDV^{TM}nanocells during each resuspension. BsAb-EDV^{TM}nanocells were resuspended to an approximate concentration of 4×10^{10} EDVs/ml in 500 μl. Counts and aggregation analysis were again performed using established techniques on the nanocyte. EGFR-His (1 mg) labeling was completed using a DyLight650 amine-reactive labeling kit (Thermo Scientific) as per the manufacturer's instructions after having been concentrated to 1.6 mg/ml using a 10 kDa spin column.

To set up samples for co-localization imaging, 2 μg EGFR-His (DyLight650) was added to 5×10^9 particles of each of the conjugated BsAb-EDV^{TM}nanocells. The resulting suspension was then incubated at RT for 30 min on a shaker at 300 rpm to allow sufficient time for recombinant EGFR binding to occur. Samples underwent 3 spin wash cycles as before to remove excess unbound labeled EGFR-His and checked for evidence of clumping resulting from BsAb-nanocell interaction with recombinant EGFR. EGFR-BsAb-nanocell suspensions were resuspended to a concentration of 0.4×10^{10} EDVs/ml. For analysis on an Olympus IX81 confocal microscope using Xcellence RT software, slides were prepared by pipetting 10 μl sample onto a clean slide that is then spread out by addition of a coverslip.

Confocal microscopy of in vitro binding of BsAb-EDV^{TM}nanocells to MDA-MB-468 cells

MDA-MB-468 cells were incubated on coverslips in the presence or absence of targeted [non-specific and ABX-EGF tandem scFv, KIH 1 (Cys), Fc-containing (Cys) and Fc-containing (CysLonglink)] and non-targeted EDV^{TM}nanocells – 7 slides total. EDV^{TM}nanocells (labeled with AF488) were added to each of 6 samples at a ratio of 10,000 EDVs per cell and the seventh was left as a "cells only" control. Plates were returned to 37°C for 3 hours which was followed by 3 washes in sterile DPBS.

Fixative volume of 500 μl, or enough to cover each coverslip, of 4% PFA was added to each of the 7 samples and left for 10 minutes for cells to become fixed. This was again followed by 3 DPBS washes. After the final wash, 500 μl DPBS was added to each well to cover the coverslips completely. An anti-EGFR mAb, 528 mAb, was labeled with AF647 to be used as a cell membrane stain; 4 μg was added directly to each sample. Wells were mixed gently and left for 10 min to allow cells to stain sufficiently. All coverslips were again washed 3 times with DPBS followed by a final wash in Milli-Q water.

Coverslips were removed from the water and placed on tissue paper cell side up to allow complete drying to occur, at which point they were mounted on clean slides using Fluka Eukitt (Sigma-Aldrich) quick-hardening mounting medium. Dry slides were stored at 4°C until confocal microscopy could be completed. Microscopy was completed on a LSM Zeiss 710 confocal using a plan-apochromat 63×/1.40 Oil DIC M27 objective and ZEN 2008 software for image formatting.

Effect of ABX-EGF tandem scFv-EDV^{TM}nanocell on tumor regression

The experiment was performed in compliance with the Australian National Health and Medical Research Council guidelines for the care and use of laboratory animals and with the approval of the EnGeneIC Animal Ethics Committee. Five-to-6 week old female Balb/C athymic nude mice were obtained from the Laboratory Animal Services at the University of Adelaide, South Australia. The animals were housed at the EnGeneIC Animal Facility under specific pathogen-free conditions.

MDA-MB-468 cells were obtained from ATCC and grown in RPMI with 10% fetal calf serum and penicillin/streptomycin. Each mouse was injected subcutaneously on the left flank with 1×10^7 cells in 100 μl of media together with 100 μl of growth factor reduced matrigel (BD Biosciences). Tumor volume was determined by measuring length (l) and width (w) and calculating volume ($V = l \times w^2 \times 0.5$). Once the tumors reached 80 – 100 mm^3 the mice were randomized into treatment groups which included 7 mice per group. The treatment groups were as follows:

- Group 1 – Saline
- Group 2 – $^{\text{Tandem scFv}}$EDV (ABX-EGF tandem scFv BsAb targeted EDV^{TM}nanocell not loaded with Doxorubicin)
- Group 3 – EDV$_{\text{Dox}}$ (Non-targeted EDV^{TM}nanocell loaded with Doxorubicin)
- Group 4 – $^{\text{Protein A/G}}$EDV$_{\text{Dox}}$ (Protein A/G linked BsAb targeted EDV^{TM}nanocell loaded with Doxorubicin)[21,22]
- Group 5 – $^{\text{Tandem scFv}}$EDV$_{\text{Dox}}$ (ABX-EGF tandem scFv BsAb targeted EDV^{TM}nanocell loaded with Doxorubicin)

The amount of Doxorubicin was measured by HPLC for all loaded EDV^{TM}nanocells and determined to be 1 ± 0.1 μg per 1×10^9 EDV^{TM}nanocells (one intravenous dose); method completed as previously described.[21,22] All treatments were injected intravenously via the tail vein and administered 3 times a week for 3 weeks. Tumors were measured using a caliper 3 times a week. The mice were weighed twice a week for 3 weeks.

Disclosure of Potential Conflicts of Interest

No potential conflicts of interest were disclosed.

Acknowledgments

Acknowledgment is given to the National Biologics Facility (AIBN) for providing protein expression facilities. EnGeneIC Ltd kindly provided access to microscopy facilities and EDV^{TM}-nanocells for binding assays, in addition to completing in vivo mouse studies using the selected BsAb format. This work was performed in part at the Queensland node of the Australian National Fabrication Facility, a company established under the National Collaborative Research Infrastructure Strategy to provide nano- and micro-fabrication facilities for Australia's researchers. Additional thanks are due to CSL for the completion of DLS and The Australian Protein Analysis Facility for evaluating BsAb stability in buffer formulations.

Funding

This work was supported by an ARC Linkage Project Grant funded by the Australian Government. Karin Taylor is supported by an Australian Postgraduate Award scholarship.

References

1. Burden RE, Caswell J, Fay F, Scott CJ. Recent advances in the application of antibodies as therapeutics. Future Med Chem 2012; 4:73-86; PMID:22168165; http://dx.doi.org/10.4155/fmc.11.165
2. Yoo J-W, Irvine DJ, Discher DE, Mitragotri S. Bio-inspired, bioengineered and biomimetic drug delivery carriers. Nat Rev Drug Discov 2011; 10:521-35; PMID:21720407; http://dx.doi.org/10.1038/nrd3499
3. Elvin JG, Couston RG, van der Walle CF. Therapeutic antibodies: Market considerations, disease targets and bioprocessing. Int J Pharm 2013; 440:83-98; PMID:22227342; http://dx.doi.org/10.1016/j.ijpharm.2011.12.039
4. Perchiacca JM, Ladiwala ARA, Bhattacharya M, Tessier PM. Aggregation-resistant domain antibodies engineered with charged mutations near the edges of the complementarity-determining regions. Protein Eng Des Sel 2012; 25:591-602; PMID:22843678; http://dx.doi.org/10.1093/protein/gzs042
5. Chames P, Baty D. Bispecific Single Domain Antibodies. New York: Springer, 2011.
6. Teillaud J-L. From whole monoclonal antibodies to single domain antibodies: think small. Methods Mol Biol 2012; 911:3-13.
7. Reichert JM, Dhimolea E. The future of antibodies as cancer drugs. Drug Discov Today 2012; 17:954-63; PMID:22561895; http://dx.doi.org/10.1016/j.drudis.2012.04.006
8. Pasquetto MV, Vecchia L, Covini D, Digilio R, Scotti C. Targeted Drug Delivery Using Immunoconjugates: Principles and Applications. J Immunother 2011; 34:611-28; PMID:21989410; http://dx.doi.org/10.1097/CJI.0b013e318234ecf5
9. Brischwein K, Schlereth B, Guller B, Steiger C, Wolf A, Lutterbuese R, Offner S, Locher M, Urbig T, Raum T, et al. MT110: A novel bispecific single-chain antibody construct with high efficacy in eradicating established tumors. Mol Immunol 2006; 43:1129-43; PMID:16139892; http://dx.doi.org/10.1016/j.molimm.2005.07.034
10. Holliger P, Hudson PJ. Engineered antibody fragments and the rise of single domains. Nat Biotechnol 2005; 23:1126-36; PMID:16151406; http://dx.doi.org/10.1038/nbt1142
11. Kontermann R. Dual targeting strategies with bispecific antibodies. mAbs 2012; 4:182-97; PMID:22453100; http://dx.doi.org/10.4161/mabs.4.2.19000
12. Zhu Z. Dual-Targeting Bispecific Antibodies as New Therapeutic Modalities for Cancer. In: Wood CR, ed. Antibody Drug Discovery. London, UK: Imperial College Press, 2011:373-408
13. May C, Sapra P, Gerber H-P. Advances in bispecific biotherapeutics for the treatment of cancer. Biochem Pharmacol 2012; 84:1105-12; PMID:22858161; http://dx.doi.org/10.1016/j.bcp.2012.07.011
14. Chames P, Baty D. Bispecific antibodies for cancer therapy The light at the end of the tunnel? MAbs 2009; 1:539-47; PMID:20073127; http://dx.doi.org/10.4161/mabs.1.6.10015
15. Byrne H, Conroy PJ, Whisstock JC, O'Kennedy RJ. A tale of two specificities: bispecific antibodies for therapeutic and diagnostic applications. Trends Biotechnol 2013; 31:621-32; PMID:24094861; http://dx.doi.org/10.1016/j.tibtech.2013.08.007
16. Lutterbuese R, Raum T, Kischel R, Hoffmann P, Mangold S, Rattel B, Friedrich M, Thomas O, Lorenczewski G, Rau D, et al. T cell-engaging BiTE antibodies specific for EGFR potently eliminate KRAS- and BRAF-mutated colorectal cancer cells. Proc Nati Acad Sci U S A 2010; 107:12605-10; PMID:20616015; http://dx.doi.org/10.1073/pnas.1000976107
17. Johnson S, Burke S, Huang L, Gorlatov S, Li H, Wang W, Zhang W, Tuaillon N, Rainey J, Barat B, et al. Effector Cell Recruitment with Novel Fv-based Dual-affinity Re-targeting Protein Leads to Potent Tumor Cytolysis and in Vivo B-cell Depletion. J Mol Biol 2010; 399:436-49; PMID:20382161; http://dx.doi.org/10.1016/j.jmb.2010.04.001
18. Atanackovic D, Reinhard H, Meyer S, Spöck S, Grob T, Luetkens T, Yousef S, Cao Y, Hildebrandt Y, Templin J, et al. The trifunctional antibody catumaxomab amplifies and shapes tumor-specific immunity when applied to gastric cancer patients in the adjuvant setting. Hum Vaccin Immunother 2013; 9:5-4; http://dx.doi.org/10.4161/hv.26065
19. Linke R, Klein A, Seimetz D. Catumaxomab: Clinical development and future directions. MAbs 2010; 2:129-36; PMID:20190561; http://dx.doi.org/10.4161/mabs.2.2.11221
20. Chelius D, Ruf P, Gruber P, Plöscher M, Liedtke R, Gansberger E, Hess J, Wasiliu M, Lindhofer H. Structural and functional characterization of the trifunctional antibody catumaxomab. MAbs 2010; 2:309-19; PMID:20418662; http://dx.doi.org/10.4161/mabs.2.3.11791
21. MacDiarmid JA, Mugridge NB, Weiss JC, Phillips L, Burn AL, Paulin RP, Haasdyk JE, Dickson KA, Brahmbhatt VN, Pattison ST, et al. Bacterially derived 400 nm particles for encapsulation and cancer cell targeting of chemotherapeutics. Cancer Cell 2007; 11:431-45; PMID:17482133; http://dx.doi.org/10.1016/j.ccr.2007.03.012
22. MacDiarmid JA, Amaro-Mugridge NB, Madrid-Weiss J, Sedliarou I, Wetzel S, Kochar K, Brahmbhatt VN, Phillips L, Pattison ST, Petti C, et al. Sequential treatment of drug-resistant tumors with targeted minicells containing siRNA or a cytotoxic drug. Nat Biotechnol 2009; 27:643-51; PMID:19561595; http://dx.doi.org/10.1038/nbt.1547
23. Torchilin VP. Recent advances with liposomes as pharmaceutical carriers. Nat Rev Drug Discov 2005; 4:145-60; PMID:15688077; http://dx.doi.org/10.1038/nrd1632
24. Ferrari M. Cancer nanotechnology: Opportunities and challenges. Nat Rev Cancer 2005; 5:161-71; PMID:15738981; http://dx.doi.org/10.1038/nrc1566
25. Webster DM, Sundaram P, Byrne ME. Injectable nanomaterials for drug delivery: Carriers, targeting moieties, and therapeutics. Eur J Pharm Biopharm 2013; 84:1-20; PMID:23313176; http://dx.doi.org/10.1016/j.ejpb.2012.12.009
26. Couvreur P. Nanoparticles in drug delivery: Past, present and future. Adv Drug Deliv Rev 2013; 65:21-3; PMID:22580334; http://dx.doi.org/10.1016/j.addr.2012.04.010
27. Lammers T, Kiessling F, Hennink WE, Storm G. Drug targeting to tumors: Principles, pitfalls and (pre-) clinical progress. J Control Release 2012; 161:175-87; PMID:21945285; http://dx.doi.org/10.1016/j.jconrel.2011.09.063
28. Steichen SD, Caldorera-Moore M, Peppas NA. A review of current nanoparticle and targeting moieties for the delivery of cancer therapeutics. Eur J Pharm Sci 2013; 48:416-27; PMID:23262059; http://dx.doi.org/10.1016/j.ejps.2012.12.006
29. Battaglia DP. Targeted Drug Delivery. Amsterdam, Netherlands: Elsevier Science Bv, 2013.
30. Peer D, Karp JM, Hong S, Farokhzad OC, Margalit R, Langer R. Nanocarriers as an emerging platform for cancer therapy. Nat Nano 2007; 2:751-60; http://dx.doi.org/10.1038/nnano.2007.387.
31. MacDiarmid JA, Brahmbhatt H. Minicells: Versatile vectors for targeted drug or si/shRNA cancer therapy. Curr Opin Biotechnol 2011; 22:909-16; PMID:21550793; http://dx.doi.org/10.1016/j.copbio.2011.04.008
32. Felice B, Prabhakaran MP, Rodriguez AP, Ramakrishna S. Drug delivery vehicles on a nano-engineering perspective. Mater Sci Eng C-Mater Biol Appl 2014; 41:178-95; PMID:24907751; http://dx.doi.org/10.1016/j.msec.2014.04.049.
33. Sanna V, Pala N, Sechi M. Targeted therapy using nanotechnology: focus on cancer. Int J Nanomed 2014; 9:467-83
34. Fay F, Scott CJ. Antibody-targeted nanoparticles for cancer therapy. Immunotherapy 2011; 3:381-94; PMID:21395380; http://dx.doi.org/10.2217/imt.11.5
35. Geers B, De Wever O, Demeester J, Bracke M, De Smedt SC, Lentacker I. Targeted Liposome-Loaded Microbubbles for Cell-Specific Ultrasound-Triggered Drug Delivery. Small 2013; 9:4027-35; PMID:23737360; http://dx.doi.org/10.1002/smll.201300161
36. Yang LL, Mao H, Wang YA, Cao ZH, Peng XH, Wang XX, Duan HW, Ni CC, Yuan QG, Adams G, et al. Single Chain Epidermal Growth Factor Receptor Antibody Conjugated Nanoparticles for in vivo Tumor Targeting and Imaging. Small 2009; 5:235-43; PMID:19089838; http://dx.doi.org/10.1002/smll.200800714
37. Goodall S, Howard CB, Jones ML, Munro T, Jia Z, Monteiro MJ, Mahler S. An EGFR Targeting Nanoparticle Self Assembled from a Thermoresponsive Polymer. J Chem Technol Biotechnol 2014; 10.1002/jctb.4509
38. Bertrand N, Wu J, Xu XY, Kamaly N, Farokhzad OC. Cancer nanotechnology: The impact of passive and active targeting in the era of modern cancer biology. Adv Drug Deliv Rev 2014; 66:2-25; PMID:24270007; http://dx.doi.org/10.1016/j.addr.2013.11.009
39. Ellerman D, Scheer JM. Generation of Bispecific Antibodies by Chemical Conjugation. New York: Springer, 2011
40. Holliger P, Prospero T, Winter G. DIABODIES - SMALL BIVALENT AND BISPECIFIC ANTIBODY FRAGMENTS. Proc Nati Acad Sci U S A 1993; 90:6444-8; PMID:8341653; http://dx.doi.org/10.1073/pnas.90.14.6444
41. Muller D, Kontermann RE. Diabodies, Single-Chain Diabodies, and Their Derivatives. New York: Springer, 2011.
42. Kontermann RE. Bispecific Antibodies. New York: Springer, 2011, 1-373.
43. Moore PA, Zhang WJ, Rainey GJ, Burke S, Li H, Huang L, Gorlatov S, Veri MC, Aggarwal S, Yang YH, et al. Application of dual affinity retargeting molecules to achieve optimal redirected T-cell killing of B-cell lymphoma. Blood 2011; 117:4542-51; PMID:21300981; http://dx.doi.org/10.1182/blood-2010-09-306449
44. Wozniak-Knopp G, Bartl S, Bauer A, Mostageer M, Woisetschlager M, Antes B, Ettl K, Kainer M, Weberhofer G, Wiederkum S, et al. Introducing antigen-binding sites in structural loops of immunoglobulin constant domains: Fc fragments with engineered HER2/neu-binding sites and antibody properties. Protein Eng Des Sel 2010; 23:289-97; PMID:20150180; http://dx.doi.org/10.1093/protein/gzq005
45. Wang L, He YR, Zhang G, Ma J, Liu CZ, He W, Wang W, Han HM, Boruah BM, Gao B. Retargeting T Cells for HER2-Positive Tumor Killing by a Bispecific Fv-Fc Antibody. PLoS ONE 2013; 8(9):e75589; PMID:24086580; doi:10.1371/journal.pone.0075589
46. Enever C, Batuwangala T, Plummer C, Sepp A. Next generation immunotherapeutics—honing the magic bullet. Curr Opin Biotechnol 2009; 20:405-11; PMID:19709876; http://dx.doi.org/10.1016/j.copbio.2009.07.002
47. Presta LG. Molecular engineering and design of therapeutic antibodies. Curr Opin Immunol 2008; 20:460-70; PMID:18656541; http://dx.doi.org/10.1016/j.coi.2008.06.012
48. Boonstra J, Rijken P, Humbel B, Cremers F, Verkleij A, Henegouwen PVE. THE EPIDERMAL GROWTH-FACTOR. Cell Biol Int 1995; 19:413-30; PMID:7640657; http://dx.doi.org/10.1006/cbir.1995.1086
49. Grunwald V, Hidalgo M. The epidermal growth factor receptor: A new target for anticancer therapy. Curr Problems in Cancer 2002; 26:109-64; PMID:12085086; http://dx.doi.org/10.1067/mcn.2002.125874
50. Mendelsohn J, Baselga J. Epidermal growth factor receptor targeting in cancer. Semin Oncol 2006;

33:369-85; PMID:16890793; http://dx.doi.org/10.1053/j.seminoncol.2006.04.003
51. Cohenuram M, Saif MW. Panitumumab the first fully human monoclonal antibody: from the bench to the clinic. Anti-Cancer Drugs 2007; 18:7-15; PMID:17159497; http://dx.doi.org/10.1097/CAD.0b013e32800feecb
52. Gemmete JJ, Mukherji SK. Panitumumab (Vectibix). Am J Neuroradiol 2011; 32:1002-3; PMID:21596817; http://dx.doi.org/10.3174/ajnr.A2601
53. Jakobovits A, Amado RG, Yang X, Roskos L, Schwab G. From XenoMouse technology to panitumumab, the first fully human antibody product from transgenic mice. Nat Biotechnol 2007; 25:1134-43; PMID:17921999; http://dx.doi.org/10.1038/nbt1337
54. Zhu JW. Mammalian cell protein expression for biopharmaceutical production. Biotechnol Adv 2012; 30:1158-70; PMID:21968146; http://dx.doi.org/10.1016/j.biotechadv.2011.08.022
55. Dinnis DM, James DC. Engineering mammalian cell factories for improved recombinant monoclonal antibody production: Lessons from nature? Biotechnol Bioeng 2005; 91:180-9; PMID:15880827; http://dx.doi.org/10.1002/bit.20499
56. Metz S, Panke C, Haas AK, Schanzer J, Lau W, Croasdale R, Hoffmann E, Schneider B, Auer J, Gassner C, et al. Bispecific antibody derivatives with restricted binding functionalities that are activated by proteolytic processing. Protein Eng Des Sel 2012; 25:571-80; http://dx.doi.org/10.1093/protein/gzs064
57. Feige MJ, Groscurth S, Marcinowski M, Shimizu Y, Kessler H, Hendershot LM, Buchner J. An Unfolded C (H)1 Domain Controls the Assembly and Secretion of IgG Antibodies. Molecular Cell 2009; 34:569-79; PMID:19524537; http://dx.doi.org/10.1016/j.molcel.2009.04.028
58. Yang XD, Jia XC, Corvalan JRF, Wang P, Davis CG, Jakobovits A. Eradication of established tumors by a fully human monoclonal antibody to the epidermal growth factor receptor without concomitant chemotherapy. Cancer Res 1999; 59:1236-43; PMID:10096554
59. Mendez MJ, Green LL, Corvalan JRF, Jia XC, MaynardCurrie CE, Yang XD, Gallo ML, Louie DM, Lee DV, Erickson KL, et al. Functional transplant of megabase human immunoglobulin loci recapitulates human antibody response in mice. Nat Genet 1997; 15:146-56; PMID:9020839; http://dx.doi.org/10.1038/ng0297-146
60. Hobbs SK, Monsky WL, Yuan F, Roberts WG, Griffith L, Torchilin VP, Jain RK. Regulation of transport pathways in tumor vessels: Role of tumor type and microenvironment. Proc Nati Acad Sci U S A 1998; 95:4607-12; PMID:9539785; http://dx.doi.org/10.1073/pnas.95.8.4607
61. Yuan F, Leunig M, Huang SK, Berk DA, Papahadjopoulos D, Jain RK. Microvascular permeability and interstitial penetration of sterically stabilized (stealth) liposomes in a human tumor xenograft. Cancer Res 1994; 54:3352-6; PMID:8012948
62. Reichert JM. Antibodies to watch in 2013: Mid-year update. MAbs 2013; 5:513-7; PMID:23727858; http://dx.doi.org/10.4161/mabs.24990
63. Merchant AM, Zhu ZP, Yuan JQ, Goddard A, Adams CW, Presta LG, Carter P. An efficient route to human bispecific IgG. Nat Biotechnol 1998; 16:677-81; PMID:9661204; http://dx.doi.org/10.1038/nbt0798-677
64. Mabry R, Gilbertson DG, Frank A, Vu T, Ardourel D, Ostrander C, Stevens B, Julien S, Franke S, Meengs B, et al. A dual-targeting PDGFR beta/VEGF-A molecule assembled from stable antibody fragments demonstrates anti-angiogenic activity in vitro and in vivo. mAbs 2010; 2:20-34; PMID:20065654; http://dx.doi.org/10.4161/mabs.2.1.10498
65. Ridgway JBB, Presta LG, Carter P. 'Knobs-into-holes' engineering of antibody C(H)3 domains for heavy chain heterodimerization. Protein Eng 1996; 9:617-21; PMID:8844834; http://dx.doi.org/10.1093/protein/9.7.617
66. Zhu ZP, Presta LG, Zapata G, Carter P. Remodeling domain interfaces to enhance heterodimer formation. Protein Sci 1997; 6:781-8; PMID:9098887; http://dx.doi.org/10.1002/pro.5560060404
67. Labrijn AF, Aalberse RC, Schuurman J. When binding is enough: nonactivating antibody formats. Curr Opin Immunol 2008; 20:479-85; PMID:18577454; http://dx.doi.org/10.1016/j.coi.2008.05.010
68. Jendreyko N. Intradiabodies, Bispecific, Tetravalent Antibodies for the Simultaneous Functional Knockout of Two Cell Surface Receptors. J Biol Chem 2003; 278:47812-9; PMID:12947084; http://dx.doi.org/10.1074/jbc.M307002200
69. Abou-Nassar K, Brown JR. Novel agents for the treatment of chronic lymphocytic leukemia. Clin Adv Hematol Oncol : H&O 2010; 8:886-95.
70. Lee CC, Perchiacca JM, Tessier PM. Toward aggregation-resistant antibodies by design. Trends Biotechnol 2013; 31:612-20; PMID:23932102; http://dx.doi.org/10.1016/j.tibtech.2013.07.002
71. Miller BR, Demarest SJ, Lugovskoy A, Huang F, Wu XF, Snyder WB, Croner LJ, Wang N, Amatucci A, Michaelson JS, et al. Stability engineering of scFvs for the development of bispecific and multivalent antibodies. Protein Eng Des Sel 2010; 23:549-57; PMID:20457695; http://dx.doi.org/10.1093/protein/gzq028
72. Demarest SJ, Glaser SM. Antibody therapeutics, antibody engineering, and the merits of protein stability. Curr Opin Drug Discov Dev 2008; 11:675-87.
73. Schanzer J, Jekle A, Nezu J, Lochner A, Croasdale R, Dioszegi M, Zhang J, Hoffmann E, Dormeyer W, Stracke J, et al. Development of Tetravalent, Bispecific CCR5 Antibodies with Antiviral Activity against CCR5 Monoclonal Antibody-Resistant HIV-1 Strains. Antimicrob Agents Chemother 2011; 55:2369-78; PMID:21300827; http://dx.doi.org/10.1128/AAC.00215-10
74. Mabry R, Lewis KE, Moore M, McKernan PA, Bukowski TR, Bontadelli K, Brender T, Okada S, Lum K, West J, et al. Engineering of stable bispecific antibodies targeting IL-17A and IL-23. Protein Eng Design Sel 2009; 23:115-27; http://dx.doi.org/10.1093/protein/gzp073
75. Moore GL, Bautista C, Pong E, Nguyen D-HT, Jacinto J, Eivazi A, Muchhal US, Karki S, Chu SY, Lazar GA. A novel bispecific antibody format enables simultaneous bivalent and monovalent co-engagement of distinct target antigens. mAbs 2011; 3:546-57; PMID:22123055; http://dx.doi.org/10.4161/mabs.3.6.18123
76. McAleese F, Eser M. RECRUIT-TandAbs (R): harnessing the immune system to kill cancer cells. Future Oncol 2012; 8:687-95; PMID:22764766; http://dx.doi.org/10.2217/fon.12.54
77. Rajkovic E, Hucke C, Knackmuss S, Molkenthin V, Reusch U, Legall F, Little M. Recruit-TandAbs: Engaging immune cells to kill cancer cells AFM13: A bispecific tetravalent TandAb for treating Hodgkin Lymphoma. 11th International Conference on Malignant Lymphoma 15-18 June 2011. Lugano (Switzerland): Ann Oncol 2011:240-1
78. Adams TE, Koziolek EJ, Hoyne PH, Bentley JD, Lu L, Lovrecz G, Ward CW, Lee FT, Scott AM, Nash AD, et al. A truncated soluble epidermal growth factor receptor-Fc fusion ligand trap displays anti-tumour activity in vivo. Growth Factors 2009; 27:141-54; PMID:19333814; http://dx.doi.org/10.1080/08977190902843565
79. Morrison SL. Cloning, expression, and modification of antibody V regions. Curr Proto Immunol 2002; Chapter 2:Unit 2.12; PMID:18432877; doi:10.1002/0471142735.im0212s47
80. Atwell S, Ridgway JB, Wells JA, Carter P. Stable heterodimers from remodeling the domain interface of a homodimer using a phage display library. J Mol Biol 1997; 270:26-35; PMID:9231898; http://dx.doi.org/10.1006/jmbi.1997.1116
81. Jones ML, Seldone T, Smede M, Linville A, Chin DY, Barnard R, Mahler SM, Munster D, Hart D, Gray PP, et al. A method for rapid, ligation-independent reformatting of recombinant monoclonal antibodies. J Immunol Methods 2010; 354:85-90; PMID:20153332; http://dx.doi.org/10.1016/j.jim.2010.02.001
82. Codamo J, Hou JJC, Hughes BS, Gray PP, Munro TP. Efficient mAb production in CHO cells incorporating PEI-mediated transfection, mild hypothermia and the co-expression of XBP-1. J Chem Technol Biotechnol 2011; 86:923-34; http://dx.doi.org/10.1002/jctb.2572